Int J Theor Phys (2009) 48: 1781–1789
DOI 10.1007/s10773-009-9949-5

Cluster State Entanglement of Semiconductor Quantum Dots Based on Faraday Rotation

Hua Wei · W.L. Yang · Fei Zhou · Ranran Fang · Xiao-Long Zhang

Received: 13 November 2008 / Accepted: 16 January 2009 / Published online: 30 January 2009

Abstract We propose a scheme for a large-scale cluster state preparation of single-charged semiconductor quantum dots utilizing Faraday rotation. Without interaction between quantum dots, the exciton induced Faraday rotation could distribute the spatially separate quantum dots into a quantum network assisted by cavity QED. We obtain the corresponding parameters from the numerical simulation based on the input-output process for the required Faraday rotation and some discussion is made in view of experimental feasibility.

Keywords Quantum entanglement · Quantum dots · Faraday rotation

1 Introduction

Entanglement is a unique character to support some specially efficient abilities in quantum information processing (QIP). Various quantum entangled states play crucial role in QIP. We will focus on cluster states in the present paper, which is a kind of entanglement resource processed in one-way condition and merely need a sequence of single-qubit operations and projective measurements to complete different functions in algorithm [1–4]. We noticed that, four-qubit cluster state of photons had been widely investigated experimentally [5–11] for Grover search, for violation of Bell inequality, for difference of entanglement from GHZ state, for quantum games, for the Deutsch's algorithm and for the one-way QIP in decoherence-free subspace. In contrast to the preparation of cluster state with flying qubits

H. Wei (✉) · X.-L. Zhang
Center for Modern Physics and Department of Physics, Chongqing University, Chongqing 400044, China
e-mail: huawei.hw@gmail.com

H. Wei · W.L. Yang · F. Zhou
State Key Laboratory of Magnetic Resonance and Atomic and Molecular Physics, Wuhan Institute of Physics and Mathematics, Chinese Academy of Sciences, Wuhan 430071, China

R. Fang
College of Mathematics and Physics, Chongqing University of Posts and Telecommunications, Chongqing 400065, China

[12–16], the stationary qubits, such as quantum dots, are preferable to store quantum information for longer time and are easy to be controlled.

On the other hand, as for future possible systematic integration, solid-state physical devices based on semiconductor system have superiority in combination with the sophisticated microsystem engineering at nanometer-scale and the artificial creation of quantum confinement with developed semiconductor processing techniques. There are many schemes in solid-state systems for the cluster state preparation, which mostly depend on topological structure [17], single-photon interference [18–20], joint measurement on two qubits [21, 22], additional single-qubit operations on the qubits [23, 24] or direct two-qubit coupling [25–27]. In this paper, we focus on semiconductor quantum dots (QDs) [28], with charge carriers in three dimensions, which is considered as a promising candidate system for large-scale QIP. Concretely speaking, we need the microcavity-embedded single-charged QD (i.e., only one excess electron in the conduction band of the QD). The spin state of the single-charged QD can be coherently operated by local the electromagnetic field [29–34], but for the distributed QIP, we prefer to use the nonlocal interactions between the photon and single-charged QDs for a quantum network [35–38]. We will show that the exciton induced Faraday rotation makes the spatially separate QDs into a distributed quantum network, assisted by cavity QED technology.

The present paper is to generate large-scale cluster state with single-charged QDs employing Faraday rotation, where each microcavity-embedded single-charged QD will complete the Faraday rotation triggered by the interaction between the photon and the QD. From the input-output process of the cavity-embedded QD system, we could determine the angle of the Faraday rotation by some pertinent parameters.

The paper is arranged as follows: In Sect. 2, we explain the Faraday rotation in the cavity-embedded QD system and show our scheme in detail how to prepare the cluster state based on Faraday rotation and single-photon detectors in QD arrays. In Sect. 3, a brief discussion is made for experimental feasibility. We present in Appendix an analytical expression as well as an exact numerical simulation for the controllable angle of the Faraday rotation.

2 Faraday Rotation in the Cavity-Embedded QD System

2.1 The Photon Interacts with a Cavity-Embedded QD

The single-charged QD, with a single excess electron in the conduction band, can be realized by tuning the gate voltage in the leads to make the Fermi energy (or say, the electrochemical potential level) of both the source and drain reservoirs match the first unoccupied single-charged state in the QD. As a result, an electron can be resonantly tunneled into the QD and will not escape because of the Coulomb blockade [39, 40].

In a nearly spherical QD of zincblende or wurtzite material, the valence states are nearly degenerate. In our scheme, we use some special QDs, such as GaAs/Al(Ga)As, in which for different energy levels of J_z, there are large energy splitting due to the low symmetry of 2D or 0D structures. Concretely speaking, the order of the energy splitting for both the heavy hole band $J_z = \pm 3/2$ and the light hole band $J_z = \pm 1/2$ for GaAs/Al(Ga)As is of tens of meV, which is big enough for the selective pulse with long time duration to exactly couple the transition between the heavy hole levels $J_z = \pm 3/2$ and the conduction band levels $S_z = \pm 1/2$, while no transition regarding the light hole levels $J_z = \pm 1/2$ due to large detuning.

More specifically, for the selective photon pulse with energy $\hbar\omega$, the selection rule and Pauli exclusion principle only allow the transition between the level $J_z = 3/2$ and the level

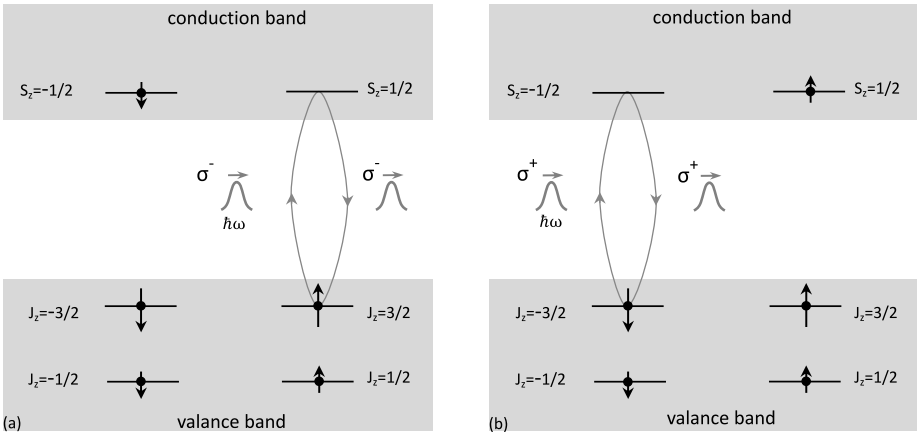

Fig. 1 Schematic virtual process in a cavity-embedded single-charged QD excited by a single-photon. The energy $\hbar\omega$ of the selective photon pulse, equal to the energy between the conduction band ($S_z = \pm 1/2$) and valence band ($J_z = \pm 3/2$), can produce a single exciton. Only two conditions are allowed under the selection rule and Pauli exclusion principle. (**a**) The transition from $J_z = 3/2$ to $S_z = 1/2$ is excited by $|\sigma^-\rangle$ polarized photon if the spin of the single-charged QD is in $|\downarrow\rangle$ and (**b**) the transition from $J_z = -3/2$ to $S_z = -1/2$ is triggered by $|\sigma^+\rangle$ polarized photon if the single-charged QD is in $|\uparrow\rangle$. The emitted photon has the same polarization as the absorbed one

$S_z = 1/2$ by a $|\sigma^-\rangle$ polarized photon if the spin state of the single-charged QD is in $|\downarrow\rangle$, while the $|\sigma^+\rangle$ polarized photon can not 'feel' the QD (i.e., the empty cavity) and thereby has not interaction with the QD, as shown in Fig. 1. On the contrary, the spin state $|\uparrow\rangle$ of the single-charged QD only allow the $|\sigma^+\rangle$ polarized photon pulse which yields the transition $J_z = -3/2 \leftrightarrow S_z = -1/2$, but $|\sigma^-\rangle$ polarized photon will not work. The transition will lead to an exciton.

We consider the cavity with large decay rate so that for a single photon moving in and out of the cavity, the above mentioned excitation only occurs virtually and leaves a Faraday rotation in the system. Concretely speaking, a phase rotation $e^{i\Phi_h}$ appears regarding the electron-heavy hole pair due to the $|\uparrow\rangle$ of the single-charged QD and the $|\sigma^+\rangle$ polarized input photon or $|\downarrow\rangle$ of the QD with $|\sigma^-\rangle$ polarized input photon, but in an 'empty cavity', the phase shift term $e^{i\Phi_0}$ comes from the case of $|\uparrow\rangle$ of the single-charged QD with a $|\sigma^-\rangle$ polarized input photon or $|\downarrow\rangle$ of the QD with $|\sigma^+\rangle$ polarized input photon. We will present the mathematical details regarding the Faraday rotation in Appendix.

The spin polarization of the single-charged QD is initialized in $(|\uparrow\rangle + |\downarrow\rangle)/\sqrt{2}$ and the state of the single-photon pulse is $|h\rangle$. We use the definition $|h\rangle = (|\sigma^+\rangle + |\sigma^-\rangle)/\sqrt{2}$ and $|v\rangle = i(|\sigma^+\rangle - |\sigma^-\rangle)/\sqrt{2}$ throughout the paper. The whole process of the interaction between the photon and the microcavity-embedded single-charged QD system can be written as,

$$
\begin{aligned}
|\Psi(0)\rangle &= |h\rangle \otimes \frac{|\uparrow\rangle + |\downarrow\rangle}{\sqrt{2}} \\
&\xrightarrow{\text{virtual process}} |\Psi\rangle = \frac{1}{2}\Big[e^{i\Phi_h}(|\uparrow\rangle|\sigma^+\rangle + |\downarrow\rangle|\sigma^-\rangle) + e^{i\Phi_0}(|\uparrow\rangle|\sigma^-\rangle + |\downarrow\rangle|\sigma^+\rangle)\Big] \qquad (1) \\
&= \frac{e^{i(\Phi_h+\Phi_0)/2}}{\sqrt{2}}\Big(|\Phi_f\rangle|\uparrow\rangle + |-\Phi_f\rangle|\downarrow\rangle\Big),
\end{aligned}
$$

where we define $|\Phi_f\rangle = (e^{i\Phi_f}|\sigma^+\rangle + e^{-i\Phi_f}|\sigma^-\rangle)/\sqrt{2}$, and $\Phi_f = (\Phi_h - \Phi_0)/2$ is the corresponding angle of the Faraday rotation.

2.2 The Photon Interacts with Two Cavity-Embedded QDs

In our scheme, the interactions between QDs are connected by the flying photons. The $|h\rangle$-polarized photon passes through two cavity-embedded QDs, i.e., Cavity-QD A and Cavity-QD B, sequentially, as shown in Fig. 2. After going through a 45° polarizer (P_{45}), the photon reaches the detector. The interaction of the photon with each cavity-embedded dot is identical to the case in (1). The initial states of the photon and the single-charged QDs are also prepared into $|h\rangle$ and $(|\uparrow\rangle + |\downarrow\rangle)/\sqrt{2}$, respectively. The complete operations can be described as follows,

$$
\begin{aligned}
|\Psi(0)\rangle &= |h\rangle \otimes \left(\frac{|\uparrow\rangle + |\downarrow\rangle}{\sqrt{2}}\right)_A \otimes \left(\frac{|\uparrow\rangle + |\downarrow\rangle}{\sqrt{2}}\right)_B \\
\xrightarrow{A} |\Psi\rangle_A &= \frac{1}{2}\Big[\big(e^{i\Phi_h^A}|\uparrow\rangle_A + e^{i\Phi_0^A}|\downarrow\rangle_A\big)|\sigma^+\rangle + \big(e^{i\Phi_h^A}|\downarrow\rangle_A + e^{i\Phi_0^A}|\uparrow\rangle_A\big)|\sigma^-\rangle\Big] \\
&\quad \otimes \left(\frac{|\uparrow\rangle + |\downarrow\rangle}{\sqrt{2}}\right)_B \\
\xrightarrow{B} |\Psi\rangle_{AB} &= \frac{1}{2\sqrt{2}}\Big[\big(e^{i\Phi_h^A}|\uparrow\rangle_A + e^{i\Phi_0^A}|\downarrow\rangle_A\big)\big(e^{i\Phi_h^B}|\sigma^+\rangle|\uparrow\rangle_B + e^{i\Phi_0^B}|\sigma^+\rangle|\downarrow\rangle_B\big) \\
&\quad + \big(e^{i\Phi_h^A}|\downarrow\rangle_A + e^{i\Phi_0^A}|\uparrow\rangle_A\big)\big(e^{i\Phi_0^B}|\sigma^-\rangle|\uparrow\rangle_B + e^{i\Phi_h^B}|\sigma^-\rangle|\downarrow\rangle_B\big)\Big] \\
&= \frac{1}{2\sqrt{2}}\Big[\big(e^{i(\Phi_h^A+\Phi_h^B)}|\sigma^+\rangle + e^{i(\Phi_0^A+\Phi_0^B)}|\sigma^-\rangle\big)|\uparrow\rangle_A|\uparrow\rangle_B \\
&\quad + \big(e^{i(\Phi_0^A+\Phi_0^B)}|\sigma^+\rangle + e^{i(\Phi_h^A+\Phi_h^B)}|\sigma^-\rangle\big)|\downarrow\rangle_A|\downarrow\rangle_B \\
&\quad + \big(e^{i(\Phi_h^A+\Phi_0^B)}|\sigma^+\rangle + e^{i(\Phi_0^A+\Phi_h^B)}|\sigma^-\rangle\big)|\uparrow\rangle_A|\downarrow\rangle_B \\
&\quad + \big(e^{i(\Phi_0^A+\Phi_h^B)}|\sigma^+\rangle + e^{i(\Phi_h^A+\Phi_0^B)}|\sigma^-\rangle\big)|\downarrow\rangle_A|\uparrow\rangle_B\Big] \\
&= \frac{e^{i(\Phi_h^A+\Phi_0^A)/2}e^{i(\Phi_h^B+\Phi_0^B)/2}}{2}\Big[\big|\Phi_f^A + \Phi_f^B\big\rangle|\uparrow\rangle_A|\uparrow\rangle_B + \big|-\Phi_f^A - \Phi_f^B\big\rangle|\downarrow\rangle_A|\downarrow\rangle_B \\
&\quad + \big|\Phi_f^A - \Phi_f^B\big\rangle|\uparrow\rangle_A|\downarrow\rangle_B + \big|-\Phi_f^A + \Phi_f^B\big\rangle|\downarrow\rangle_A|\uparrow\rangle_B\Big],
\end{aligned}
\tag{2}
$$

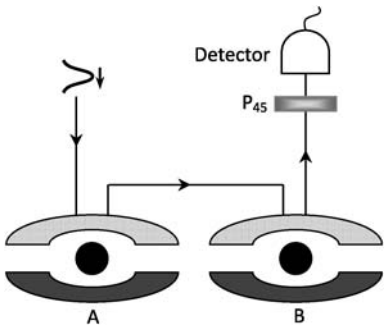

Fig. 2 Schematic setup for the interaction of a single photon with two cavity-embedded QDs sequentially. A $|h\rangle$-polarized single-photon pulse interacts respectively with the QDs **A** and **B**, followed by a 45° polarizer (P_{45}), and then would be measured by a detector. The cavity is supposed to be with a perfectly reflective wall and with a partially reflective wall

where the corresponding angels of the Faraday rotation are $\Phi_f^A = (\Phi_h^A - \Phi_0^A)/2$ and $\Phi_f^B = (\Phi_h^B - \Phi_0^B)/2$, respectively. And the definition $|\Phi_f\rangle$ has the same form with the previous section, for example, $|\Phi_f^A + \Phi_f^B\rangle = (e^{i(\Phi_f^A+\Phi_f^B)}|\sigma^+\rangle + e^{-i(\Phi_f^A+\Phi_f^B)}|\sigma^-\rangle)/\sqrt{2}$. We will show in the Appendix that suitable parameters of the cavity-embedded single-charged QD system can be found to control the corresponding Faraday rotation into $\Phi_f^A = \Phi_f^B = \pi/4$, the results in (2) can be simplified into (with the global phase omitted)

$$\begin{aligned}
&\xrightarrow{\Phi_f^A=\Phi_f^B=\pi/4} |\Psi\rangle_{AB} = \frac{1}{2}\Big[|v\rangle|\uparrow\rangle_A|\uparrow\rangle_B - |v\rangle|\downarrow\rangle_A|\downarrow\rangle_B + |h\rangle|\uparrow\rangle_A|\downarrow\rangle_B + |h\rangle|\downarrow\rangle_A|\uparrow\rangle_B\Big] \\
&\xrightarrow{\mathrm{P}_{45}} |\Psi\rangle_{AB} = \frac{|h\rangle + |v\rangle}{\sqrt{2}} \otimes \frac{1}{2}(|\uparrow\rangle_A + |\downarrow\rangle_A\sigma_z^B) \otimes (|\uparrow\rangle_B + |\downarrow\rangle_B) \qquad (3) \\
&\xrightarrow{\text{successful detection}} |\Psi\rangle_{AB} = \frac{1}{2}(|\uparrow\rangle_A + |\downarrow\rangle_A\sigma_z^B) \otimes (|\uparrow\rangle_B + |\downarrow\rangle_B).
\end{aligned}$$

After the photon passes through the 45° polarizer and then gets measured by the detector successfully, a standard two-qubit cluster state [1–4] between the two QDs is generated.

2.3 Extension to N Qubits

Our scheme can be extended to N qubits directly, as shown in Fig. 3. The initial spin state of each cavity-embedded single-charged QD system is prepared in $(|\uparrow\rangle + |\downarrow\rangle)/\sqrt{2}$, and the single-photon is set in linear polarization $|h\rangle$. It must be mentioned that each interaction of the single-photon with the cavity-embedded single-charged QD system is identical to the case in Fig. 2 and (3). There are two optical paths, one is along the direction 1-2-P_{45}-D (i.e.,

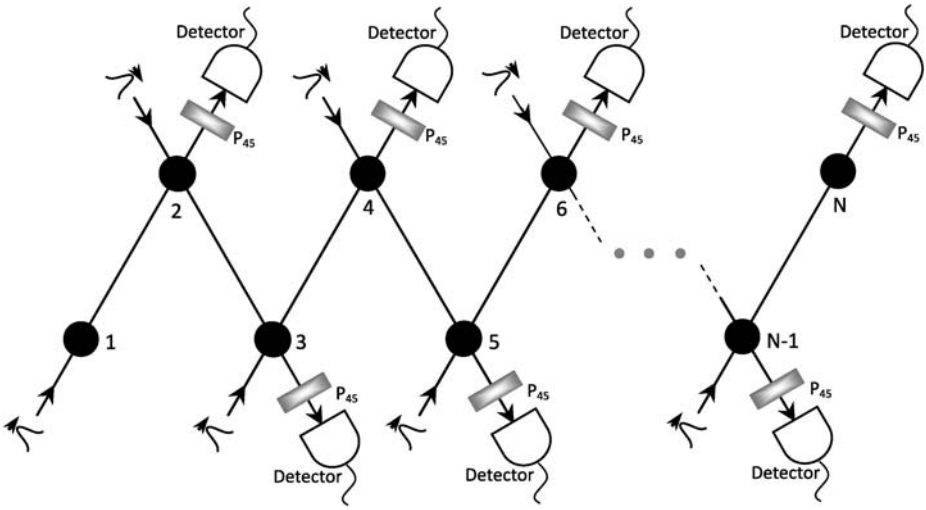

Fig. 3 Schematic setup for scalable cluster state generation with N qubits. We first have the optical paths 1-2-P_{45}-D (i.e., Detector), 3-4-P_{45}-D, ..., and $(N-1)$-N-P_{45}-D working synchronously, and then have 2-3-P_{45}-D, 4-5-P_{45}-D, ..., and $(N-2)$-$(N-1)$-P_{45}-D working synchronously. As a result, the standard N-qubit cluster state $\frac{1}{2^{N/2}}\bigotimes_{a=1}^{N}(|\downarrow\rangle_a\sigma_z^{(a+1)} + |\uparrow\rangle_a)$ could be generated

Detector), 3-4-P_{45}-D, ..., and $(N-1)$-N-P_{45}-D, the system turns into

$$\begin{aligned}&\frac{1}{2^{N/2}}(|\uparrow\rangle_1+|\downarrow\rangle_1\sigma_z^2)\otimes(|\uparrow\rangle_2+|\downarrow\rangle_2)\\&\quad\otimes(|\uparrow\rangle_3+|\downarrow\rangle_3\sigma_z^4)\otimes(|\uparrow\rangle_4+|\downarrow\rangle_4)\\&\quad\cdots\\&\quad\otimes(|\uparrow\rangle_{N-3}+|\downarrow\rangle_{N-3}\sigma_z^{N-2})\otimes(|\uparrow\rangle_{N-2}+|\downarrow\rangle_{N-2})\\&\quad\otimes(|\uparrow\rangle_{N-1}+|\downarrow\rangle_{N-1}\sigma_z^{N})\otimes(|\uparrow\rangle_{N}+|\downarrow\rangle_{N}),\end{aligned}\tag{4}$$

and the other is 2-3-P_{45}-D, 4-5-P_{45}-D, ..., and (2^N-2)-(2^N-1)-P_{45}-D, the corresponding result is

$$\begin{aligned}&\frac{1}{2^{N/2}}(|\uparrow\rangle_1+|\downarrow\rangle_1\sigma_z^2)\otimes(|\uparrow\rangle_2+|\downarrow\rangle_2\sigma_z^3)\\&\quad\otimes(|\uparrow\rangle_3+|\downarrow\rangle_3\sigma_z^4)\otimes(|\uparrow\rangle_4+|\downarrow\rangle_4\sigma_z^5)\\&\quad\cdots\\&\quad\otimes(|\uparrow\rangle_{N-3}+|\downarrow\rangle_{N-3}\sigma_z^{N-2})\otimes(|\uparrow\rangle_{N-2}+|\downarrow\rangle_{N-2}\sigma_z^{N-1})\\&\quad\otimes(|\uparrow\rangle_{N-1}+|\downarrow\rangle_{N-1}\sigma_z^{N})\otimes(|\uparrow\rangle_{N}+|\downarrow\rangle_{N}).\end{aligned}\tag{5}$$

Accordingly, two operation steps are, firstly, the interactions in the first optical path direction, such as 1-2-P_{45}-D, are operated synchronously, after the successful detections for the single-photons, then the interactions in the second optical path direction, like 3-2-P_{45}-D, are synchronously started. The successful detections of the detectors indicate a standard N-qubit cluster state of QDs $\frac{1}{2^{N/2}}\bigotimes_{a=1}^{N}(|\downarrow\rangle_a\sigma_z^{(a+1)}+|\uparrow\rangle_a)$ [1–4] is completed.

3 Discussion about the Experimental Feasibility

According to the experimental parameters from recent nanocavity-embedded QD strong coupling research, the order of the cavity quality factor is 10^4, the decay rate of the exciton and the cavity mode in the photonic crystal nanocavity coupled QD system are $(\gamma,\kappa)/2\pi=(0.2,16)$ GHz [41], and the maximal coupling strength of the exciton and the photonic crystal nanocavity is $g=21.8$ GHz [42], while in a strongly coupled microdisk-QD system the coherent coupling strength between the cavity mode and the QD, and the cavity field decay rate can obtain $(g,\kappa)/2\pi=(15,1.2)$ GHz [43]. In the theoretic numerical simulation in Fig. 4 by using the results from Appendix, we made a general parameters $g/\kappa=2.0$ and $(\gamma,\kappa)/2\pi=(0.2,16)$ GHz to give the evolvement of the absolute value of reflectance $|R_g|$ and the angle of the Faraday rotation $|\Phi_f|$ following the frequency detuning Δ where we choose the cavity mode is resonant with the exciton mode.

We can learn from Fig. 4 that, after the photon interacts with the cavity-embedded QD the amplitude of a_{out} of the output photon pulse have remarkable damping in $\Delta/\kappa=\pm2.0$, while the single-photon pulse works well with $|R_g|=1$ [47–49]. Then, the parameters with the values $\{\Delta/\kappa=0.5873,\Phi_f=\pi/4,|R_g|=0.998\}$ and $\{\Delta/\kappa=-0.5874,\Phi_f=-\pi/4,|R_g|=0.998\}$ will be adopted for the cluster state initialization in our scheme. And for the selected pulse with long duration, γ should be small enough to make the long photon pulse to accomplish its complete interaction.

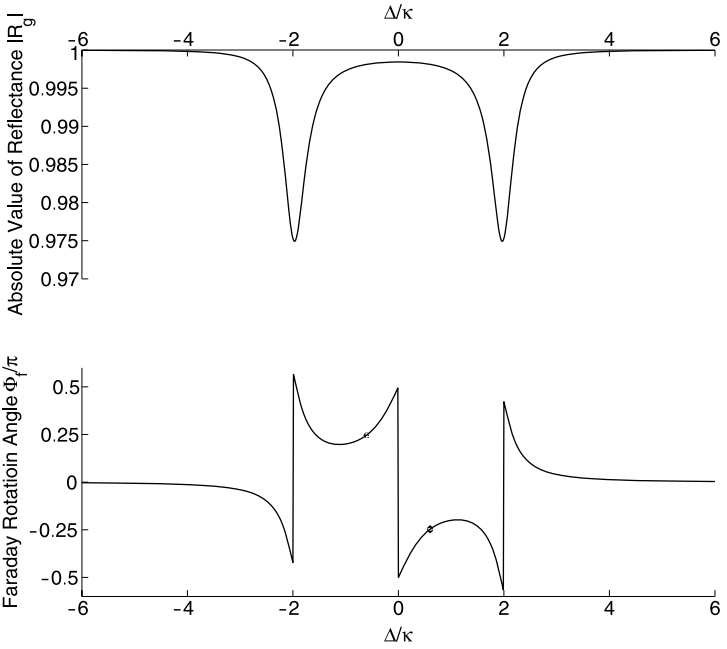

Fig. 4 Numerical simulation for the absolute value of reflective coefficient $|R_g|$ and the angle of the Faraday rotation Φ_f with respect to the detuning, $\Delta = \omega_c - \omega$, where we choose $\Delta_E = \Delta$. The ratio of the coupling strength and the cavity decay chosen here are $g/\kappa = 2.0$ and the values for $\Delta/\kappa = 0.5874$, $\Phi_f = \pi/4$, $|R_g| = 0.998$ are taken if $\pi/4$ Faraday rotation is required for the case that the single-charged QD is in $|\uparrow\rangle$, while $\Delta/\kappa = -0.5874$, $\Phi_f = -\pi/4$, $|R_g| = 0.998$ are taken when the QD is in $|\downarrow\rangle$

The currently achieved technology of deterministic single-photon source [44], with 10,000 high-quality single photons generated continuously per second, supports a fast implementation of our scheme. A realistic setup with linear optic elements, however, cannot work in a lossless way. The possible imperfection includes the photon loss, detector dark counts and the phase instability. Nevertheless, the repeat-until-success technology [45] and the successful response of the detectors could discard all events with infidelity in our scheme. Following the realization of stronger coupling between the cavity mode and the QD in near future, the wider angle of the controllable Faraday rotation is available, which will have more fruitful applications for the cavity-embedded QD system in QIP.

In summary, we have proposed a scheme for preparing the cluster state of single-charged QD arrays based on single-photon measurements and controllable Faraday rotation. It works for a distributed quantum network, which the QDs act as stationary qubits and the flying photons are used to complete the entanglement. From the analysis of the Faraday rotation, we have presented how to complete our scheme by some optimal parameters.

Acknowledgements The authors would like to thank Professor Mang Feng for valuable discussions and useful comments. This work is partly supported by National Natural Science Foundation of China under Grant Nos. 10774163 and 60490280, and also by National Fundamental Research Program of China under Grant No. 2006CB921203.

Appendix

Precise control of the Faraday rotation depends on the microcavity holding a QD. The pertinent parameters are coupling strength g between the virtual exciton and the cavity mode, cavity field decay rate κ and exciton decay rate γ [47–49].

The Hamiltonian describing the interaction between the cavity mode a and the transition operator of the exciton $\sigma_+(\sigma_-)$ in the interaction picture is

$$H_I = ig(a\sigma_+ - a^\dagger\sigma_-). \tag{6}$$

The dynamics of the system is governed by the input-output equations [46]

$$\begin{aligned} \dot{a}(t) &= -i[a(t), H_I] - (i\Delta + \kappa/2)a(t) - \sqrt{\kappa}a_{\text{in}}(t), \\ \dot{\sigma}_- &= -i[\sigma_-, H_I] - (i\Delta_E + \gamma/2)\sigma_- + f, \\ a_{\text{out}}(t) &= a_{\text{in}}(t) + \sqrt{\kappa}a(t), \end{aligned} \tag{7}$$

where $\Delta = \omega_c - \omega$ is the detuning of the cavity mode with respect to the input photon, and $\Delta_E = \omega_e - \omega$ is the frequency detuning between the QD exciton and the input photon. κ is the cavity field decay rate and γ is the QD exciton decay rate. f is a negligible term induced by the interaction between the input photon and the QD exciton which has the same order with the noise of the system to keep the commutation relations [47–49].

We can get the steady solution, after the interaction of the photon and the cavity-embedded QD system, from (7) for the reflective coefficient that

$$R_g = \frac{a_{\text{out}}}{a_{\text{in}}} = 1 - \frac{\kappa(i\Delta_E + \gamma/2)}{(i\Delta_E + \gamma/2)(i\Delta + \kappa/2) + g^2}. \tag{8}$$

As mentioned in Sect. 2, if the polarized light cannot 'feel' the QD due to the selection rules and Pauli exclusion principle, the corresponding reflection coefficient is

$$R_0 = 1 - \frac{\kappa}{i\Delta + \kappa/2}. \tag{9}$$

The exciton induced Faraday rotation comes from the difference of the phase angles between Φ_g and Φ_0, where $R_g = |R_g|e^{i\Phi_g}$, $R_0 = |R_0|e^{i\Phi_0}$, and the angle of Faraday rotation is $\Phi_f = (\Phi_g - \Phi_0)/2$. We present in Fig. 4 the numerical simulation for the absolute value of the reflective coefficient $|R_g|$ and the angle of the Faraday rotation Φ_f following the variable of the frequency detuning.

References

1. Briegel, H.J., Raussendorf, R.: Phys. Rev. Lett. **86**, 910 (2001)
2. Raussendorf, R., Briegel, H.J.: Phys. Rev. Lett. **86**, 5188 (2001)
3. Raussendorf, R., Browne, D.E., Briegel, H.J.: Phys. Rev. A **68**, 022312 (2003)
4. Van den Nest, M., Dür, W., Miyake, A., Briegel, H.J.: New J. Phys. **9**, 204 (2007)
5. Walther, P., et al.: Nature **434**, 169 (2005)
6. Walther, P., Aspelmeyer, M., Resch, K.J., Zeilinger, A.: Phys. Rev. Lett. **95**, 020403 (2005)
7. Kiesel, N., et al.: Phys. Rev. Lett. **95**, 210502 (2005)
8. Prevedel, R., Stefanov, A., Walther, P., Zeilinger, A.: New J. Phys. **9**, 205 (2007)
9. Tame, M.S., Prevedel, R., Paternostro, M., Böhi, P., Kim, M.A., Zeilinger, A.: Phys. Rev. Lett. **98**, 140501 (2007)

10. Pervelel, R., et al.: Phys. Rev. Lett. **99**, 250503 (2007)
11. Tame, M.S., Paternostro, M., Kim, M.S.: New J. Phys. **9**, 201 (2007)
12. Chen, K., et al.: Phys. Rev. Lett. **98**, 120503 (2007)
13. Vallone, G., et al.: Phys. Rev. Lett. **98**, 180502 (2007)
14. Zhang, A.-N., et al.: Phys. Rev. A **73**, 022330 (2006)
15. Nielsen, M.A.: Phys. Rev. Lett. **93**, 040503 (2004)
16. Menicucci, N.C., et al.: Phys. Rev. Lett. **97**, 110501 (2006)
17. Chen, Q., Cheng, J.H., Wang, K.L., Du, J.F.: Phys. Rev. A **73**, 012303 (2006)
18. Barrett, S.D., Kok, P.: Phys. Rev. A **71**, 060310(R) (2005)
19. Grond, J., Pötz, W.: Phys. Rev. B **77**, 165307 (2008)
20. Pötz, W.: Phys. Rev. B **77**, 035310 (2008)
21. Lim, Y.L., Barrett, S.D., Beige, A., Kok, P., Kwek, L.C.: Phys. Rev. A **73**, 012304 (2006)
22. Zhang, X.L., Gao, K.L., Feng, M.: Phys. Rev. A **75**, 034308 (2007)
23. Zhang, X.L., Feng, M., Gao, K.L.: Phys. Rev. A **73**, 014301 (2006)
24. Zhang, X.L., Gao, K.L., Feng, M.: Phys. Rev. A **74**, 024303 (2006)
25. Bodoky, F., Blaauboer, M.: Phys. Rev. A **76**, 052309 (2007)
26. D'Amico, I., Lovett, B.W., Spiller, T.P.: Phys. Rev. A **76**, 030302 (2007)
27. Yang, W.X., Zhan, Z.M., Li, J.H.: Phys. Rev. A **72**, 062108 (2005)
28. Reimann, S.M., Manninen, M.: Rev. Mod. Phys. **74**, 1283 (2002)
29. Petta, J.R., et al.: Science **309**, 2180 (2005)
30. Stinaff, E.A., et al.: Science **311**, 636 (2006)
31. Nowack, K.C., et al.: Science **318**, 1430 (2007)
32. Zhang, W.M., Wu, Y.Z., Soo, C., Feng, M.: Phys. Rev. B **76**, 165311 (2007)
33. Feng, M., An, J.H., Zhang, W.M.: J. Phys. C **19**, 326215 (2007)
34. Hai, W.H., et al.: Int. J. Theor. Phys. **39**, 1405 (2000)
35. Wei, H., Deng, Z.J., Zhang, X.L., Feng, M.: Phys. Rev. A **76**, 054304 (2007)
36. Wei, H., Yang, W.L., Deng, Z.J., Feng, M.: Phys. Rev. A **78**, 014304 (2008)
37. Wei, H., et al.: J. Phys. B **41**, 085506 (2008)
38. Xue, P., Xiao, Y.F.: Phys. Rev. Lett. **97**, 140501 (2006)
39. Van der Wiel, W.G., et al.: Rev. Mod. Phys. **75**, 1 (2003)
40. Hanson, R., et al.: Rev. Mod. Phys. **79**, 1217 (2007)
41. Fushman, I., et al.: Science **320**, 769 (2008)
42. Hennessy, K., et al.: Nature **445**, 896 (2007)
43. Srinivasan, K., Painter, O.: Nature **450**, 862 (2007)
44. Hijlkema, M., et al.: Nature Phys. **3**, 253 (2007)
45. Lim, Y.L., Beige, A., Kwek, L.C.: Phys. Rev. Lett. **95**, 030505 (2005)
46. Walls, D.F., Milburn, G.J.: Quantum Optics. Springer, Berlin, (1994)
47. Turchette, Q.A., Hood, C.J., Lange, W., Mabuchi, H., Kimble, H.J.: Phys. Rev. Lett. **75**, 4710 (1995)
48. Duan, L.-M., Kuzmich, A., Kimble, H.J.: Phys. Rev. A **67**, 032305 (2003)
49. Hu, C.Y., Young, A., O'Brien, J.L., Rarity, J.G.: arXiv:0708.2019v2 (2008)